Improved Artificial Potential Field Algorithm Based Multi-Local Minimum Solution

Riky Dwi Puriyanto, Oyas Wahyunggoro, and Adha Imam Cahyadi

***Abstract*—Artificial Potential Field (APF) is a path planning algorithm that is considered reliable to produce obstacle-free paths. One of the main drawbacks of the APF algorithm is that it is trapped at a local minimum. Some forms of local minimums are symmetrically aligned robot-obstacle-goal (SAROG) and goal non-reachable due to obstacle nearby (GNRON). Previous research resolved local minimum problems separately. In this study, the local minimum problem in the form of a single local minimum problem and a multi-local minimum problem is solved by the Improved Artificial Potential Field (I-APF) algorithm. The auxiliary function (v) was created to solve the SAROG problem. This function functions to change the resultant value of the force formed by force on each axis. In addition, GNRON is accomplished using adaptive repulsive gain and adaptive distance between the goal and current position. The I-APF algorithm is successfully used to solve local minimum problems in the form of a single local minimum and multi-local minimum. Based on the results obtained at the initial distance = 10, the average of the total trajectory (D_{trav}) generated by the I-APF algorithm is 11.93. The average E_{rg} value with a tolerance of 0.01 is 0.0077.**

***Index Terms*—artificial potential field, local minimum, SAROG, GNRON, potential function.**

I. Introduction

NAVIGATION is the main function of an automated robot in carrying out tasks. The basic components of navigation are localization, mapping, and path planning. A good path planning algorithm implemented in a robot can not only save a lot of time but also reduce capital investment to build a robot[1]. Therefore, research on path planning becomes a hot topic both among researchers.

Path planning can be categorized based on the completeness of property and the scope[2]. Depending on the completeness of the property, the path planning algorithm can be divided into a classical approach and a heuristic approach [2], [3], [4], [5]. The classical approach guarantees a solution is reached if the solution exists and can prove that the solution does not exist. The examples of the classical approach are Voronoi Diagram (VD)[6], Visibility Graph (VG)[7], Cell Decomposition (CD)[8], and Artificial Potential Field (APF)[9], [10]. The heuristic approach can produce a shorter path in a shorter time than the classical approach. However, the heuristic approach does not always guarantee to provide solutions when in a new environment and uncertainty conditions. The examples of the heuristic approach are Fuzzy Logic[11], Genetic Algorithm (GA)[12], and Neural Network (NN)[13].

Manuscript received September 19, 2020; revised July 14, 2021. The publishing process of the paper was supported by RTA 2021 Grant. We are thankful to Direktorat Penelitian UGM for their logistical support and for providing necessary guidance concerning projects.

Riky Dwi Puriyanto is PhD candidate in the Department of Electrical and Information Engineering, Universitas Gadjah Mada, Yogyakarta, Indonesia, (e-mail: riky.dp@mail.ugm.ac.id/ rikydp@ee.uad.ac.id).

Oyas Wahyunggoro is Associate Professor of Department of Electrical and Information Engineering, Universitas Gadjah Mada, Yogyakarta, Indonesia (e-mail: oyas@ugm.ac.id).

Adha Imam Cahyadi is Assistant Professor of Department of Electrical and Information Engineering, Universitas Gadjah Mada, Yogyakarta, Indonesia (e-mail: adha.imam@ugm.ac.id).

Depending on the scope, the path planning algorithm can be divided into a global approach and a local approach. A global approach generates a collision-free path based on the previous knowledge of the map. These methods have capable of finding the path or solution if it exists. Most of these methods are better used in static environments. However, they can lose effectiveness in an uncertain condition. The examples of a global approach are Neural Network (NN), Visibility Graph (VG), Voronoi Diagram (VD), and Genetic Algorithm (GA). On the other hand, a local approach uses a local sensor and the basic assumption to generate a collision-free path. This algorithm requires low computational effort so that it can be used in realtime applications. The examples of a local approach are Artificial Potential Field (APF), Virtual Force Field (VFF)[14], Virtual Force Histogram (VFH)[15], Wall Following[16], and Bug Algorithm[17], [18].

Robotic applications require a path planning algorithm that can be used in realtime. One of the reliable path planning algorithms that can be implemented in realtime is the Artificial Potential Field (APF). APF is a type of classical algorithm that can be used in realtime conditions. According to [19], the use of the heuristic approach is currently more widely used than the classical approach. However, research into classical approaches, especially APF, is still widely researched. Research conducted focuses on resolving the shortcoming of APF that are trapped in a local minimum condition[2], [20], [21], [22], [23].

Fig. 1 shows the local minimum problem that can be occurred in APF implementation. The local minimum form based on the previous research is divided into a local minimum due to the difference in force equal to zero, symmetrically aligned robot-obstacle-goal (SAROG)[24], symmetrical static object distribution (SSOD), and goal non-reachable due

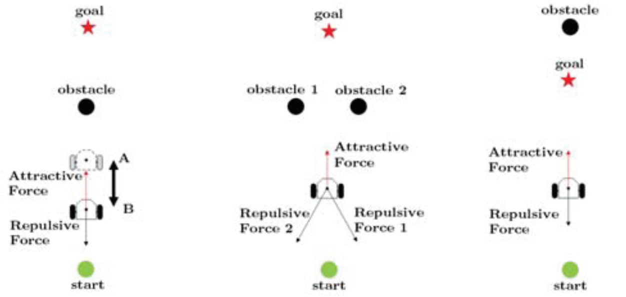

(a) SAROG (b) SSOD (c) GNRON

Fig. 1. Local minimum condition

to obstacle nearby (GNRON)[22]. Other conditions that are not an unexpected or uncertain condition, such as moving obstacles and goals, can affect the path of the robot to reach the goal. Paths that are initially optimal can turn into local minimum traps when there are unexpected conditions.

Some research explains the solution to the local minimum problem of APF. The SAROG problem was solved by [24] using a random force algorithm. Modifications of APF made by [25] in resolving GNRON problems are by multiplying the repulsive potential field function with the closest distance between the robot and the goal in n^{th} order. This method was successfully used to solve the GNRON problem in the APF algorithm. Researchers [22] use this method in testing more complex forms of obstacles. The results show the robot is trapped in a local minimum trap. Therefore, [22] added a virtual obstacle to keep the robot away from the local minimum trap.

Previous research has not fully resolved the local minimum problem. Local minimum problem solving is done on a single local minimum problem type. The path planning algorithm will face a complex environment involving minimum multi-local problems. Therefore,the primary motivation behind this work is to propose an improvement of the APF algorithm to eliminate the shortcoming of the Traditional APF (T-APF) algorithm. This research will solve the multi-local minimum problem using the Improved APF algorithm. The proposed method consists of:

1) Modification of the potential repulsive force using the sigmoid function for the switching function.
2) Modification of robot motion design by generating an auxiliary bounded input function in the total of force in the y-axis to solve SAROG problem.
3) Modification of repulsive gain parameters based on the distance of the robot to the goal to solve the GNRON problem.
4) The objective functions used to analyze the success of the path planning algorithm are the distance traveled (D_{trav}) and the error in the final position against the target position (E_{rg}).

II. Traditional Artificial Potential Field

The basic idea of the Traditional Artificial Potential Field (T-APF) path planning algorithm is to use the attractive force generated by the target to pull the robot towards the goal and the repulsive force generated by the obstacle to push the robot away from the obstacle. Both of these forces contribute to controlling the robot's motion into a collision-free path. The attractive potential field is the quadratic form given by the following equation.

$$U_{att}(q) = \frac{1}{2}\xi d^2(q, q_{goal}) \tag{1}$$

where ξ is the attractive gain parameter, $q = [x, y]^t$ is the current position of the robot, $q_{goal} = [x_g, y_g]^t$ is the coordinate of the goal, and $d(q, q_{goal}) = \|q - q_{goal}\|$ is the Euclidean distance between the robot and the goal. From (1), the attractive potential force is negative to minimize energy, as seen in (2).

$$\begin{aligned} F_{att}(q) &= -\nabla U_{att}(q) = -\frac{\partial U_{att}(q)}{\partial q} \\ F_{att}(q) &= -\xi d(q, q_{goal})\nabla(q, q_{goal}) \end{aligned} \tag{2}$$

where $\nabla(q, q_{goal}) = \frac{q - q_{goal}}{d(q, q_{goal})}$ is the gradient of the attractive potential field function.

The repulsive potential field appears when the robot is at a certain distance (r). When the robot is at a distance greater than r, the magnitude of the repulsive potential field that the robot receives is zero. The following equation gives the repulsive potential field function.

$$U_{rep.i}(q) = \begin{cases} \frac{1}{2}\eta\left(\frac{1}{d_i(q_{obs.i}, q)} - \frac{1}{r}\right)^2 & \text{if } d_i(q_{obs.i}, q) \le r \\ 0 & \text{if } d_i(q_{obs.i}, q) > r \end{cases} \tag{3}$$

with η is the repulsive gain parameter, $q_{obs} = [x_o, y_o]^t$ is the coordinate of the obstacle, r is distance affected by repulsive force, and $d_i(q_{obs.i}, q) = \|q_{obs.i} - q\|$ is the Euclidean distance between the Robot and the obstacle. The repulsive potential force can be seen in (4).

$$F_{rep.i}(q) = -\nabla U_{rep.i}(q) = -\frac{\partial U_{rep.i}(q)}{\partial q}$$

$$F_{rep.i}(q) = \begin{cases} -\eta\left(\dfrac{1}{d_i(q, q_{obs.i})} - \dfrac{1}{r}\right) \left(\dfrac{\nabla(q, q_{obs.i})}{d_i^2(q - q_{obs.i})}\right) & \text{if } d_i(q_{obs.i}, q) \le r \\ 0 & \text{if } d_i(q_{obs.i}, q) > r \end{cases} \tag{4}$$

where $\nabla(q_{obs.i}, q) = \frac{q_{obs.i} - q}{d(q_{obs.i}, q)}$ is the gradient of the repulsive potential field function. The total potential field, if there are many obstacles, can be seen in (5).

$$U_{total}(q) = U_{att}(q) + \sum_{i=1}^{n} U_{rep.i}(q) \tag{5}$$

where n is the number of obstacles. Thus, the total potential force is

$$F_{total}(q) = F_{att}(q) + \sum_{i=1}^{n} F_{rep.i}(q) \tag{6}$$

The path taken by the robot is obtained from the magnitude of the resultant force in accordance with the following equation.

$$F = \sqrt{F_x^2 + F_y^2} \tag{7}$$

where,

$$F_x(q) = -\left(\frac{dU_{att}(q)}{dx} + \frac{dU_{rep.i}(q)}{dx}\right) \tag{8}$$

$$F_y(q) = -\left(\frac{dU_{att}(q)}{dy} + \frac{dU_{rep.i}(q)}{dy}\right) \tag{9}$$

From (7), the path produced at cartesian coordinates from the initial point to the goal is obtained based on (10) and (11).

$$x_{new} = x + c\ cos(\delta) \tag{10}$$

$$y_{new} = y + c\ sin(\delta) \tag{11}$$

where c denotes the step size and $\delta = atan\frac{F_y}{F_x}$.

The T-APF path planning algorithm has a disadvantage in that it can be trapped at a local minimum. Finding the optimum point depends on the attractive and the repulsive potential field. Some of the possible conditions include:

- *Condition 1*
  If there is only an attractive potential field from a goal

(U_{att}), then $U_{T-APF} = U_{att}$. The optimum value is obtained at the goal position (q_{goal}).

- *Condition 2*
  If there is an attraction potential field (U_{att}) and a repulsive potential field of an obstacle, then $U_{T-APF} = U_{att} + U_{rep}$. When the robot moves in a symmetrical position between the robot, the obstacle, and the goal, then the minimum values are located at q_{loc}=$[x_{loc}$,$y_{loc}]^t$ and q_{goal}. Position q_{loc} is the local minimum and q_{goal} is the global minimum. When the robot is in a straight line with the bstacle and goal, the robot can be trapped at q_{loc}. This problem is called symmetrically aligned robot-obstacle-goal (SAROG).
- *Condition 3*
  If there is an attractive potential field (U_{att}) and repulsive potential field ($U_{rep.i}$) generated by two obstacles ($i = 2$) with a distance between obstacles less than 2r ($d(q_{obs.1}, q_{obs.2}) < 2r$), then $U_{T-APF} = U_{att} + U_{rep.1} + U_{rep.2}$. When the robot moves in a symmetrical position between the robot, the center of the symmetrical obstacles, and the goal, then the minimum values are located at q_{loc}=$[x_{loc}$,$y_{loc}]^t$ and q_{goal}. When the robot moves perpendicular to the q_{loc} towards q_{goal}, the robot can be trapped in the local minimum position at q_{loc}. This problem is called symmetrical static object distribution (SSOD)
- *Condition 4*
  If there is an attractive potential field of attraction (U_{att}) and a repulsive potential field (U_{rep}) of an obstacle that is close to the goal with $d(q_{goal}, q_{obs}) < r$, then $U_{APF} = U_{att} + U_{rep}$. When the robot moves in a symmetrical position between the robot, the obstacle, and the goal, then the minimum values are located at q_{loc} and $q_{newgoal}$. The minimum global position is shifted from q_{goal} to $q_{newgoal}$ due to the influence of the value of the obstacle's repulsive potential field so that the robot can be trapped in a local minimum condition. This problem is called by goal non-reachable due to obstacles nearby (GNRON).

III. Proposed Method

In this study, an Improved Artificial Potential Field (IAPF) was proposed to avoid multi-local minimum problems. The attractive potential field equation used in I-APF corresponds to (1), and the attractive potential force of I-APF based on equation from [26]. The repulsive potential field equation is modified using the sigmoid function as a switching function. For convenience, some distance parameters can be changed to the following:

- $d_i(q_{obs.i}, q) = S_{or}$
- $d_i(q, q_{goal}) = S_{rg}$
- $d_i(q_{obs.i}, q_{goal}) = S_{og}$

The proposed attractive and repulsive potential field equation can be seen in (12) and (13).

$$U_{att}(q) = \frac{1}{2}\xi S_{rg} \tag{12}$$

$$U_{rep.i}(q) = \frac{1}{2}\left(\frac{K}{S_{or}}\right) \tag{13}$$

where,

$$K = \frac{\eta}{1 + e^{m(S_{or}-r)}} \tag{14}$$

Parameter of m is the regulator of the steepness of the curve, and r is the distance affected by the repulsive potential field. The repulsive potential force based on (13) can be seen in (15).

$$F_{rep.i}(q) = -\nabla U_{rep.i}(q) = -\frac{\partial U_{rep.i}(q)}{\partial q} \tag{15}$$

Modification of the switching function to become a sigmoid function is to produce a smoother change in the total potential field around the obstacle. This change in condition is useful for predicting the potential force to generate collision-free paths. The resulting total potential force value serves to produce the next coordinate based on equation (10) dan (11). Equation (15) needs to be modified to solve the SAROG problem by producing an auxiliary function (v) to change the direction of the potential force. Besides, the total potential field value needs to be adjusted to the distance between the goal and obstacle to solving the GNRON problem. The comparison of the potential field shapes of the T-APF and I-APF can be seen in Fig. 2 (a) and (b).

Attractive gain (ξ) and repulsive gain parameters (η) affect the formation of a potential field in the robot's environment. The greater the attractive gain value with a constant repulsive gain value, the smaller the repulsive potential field around the obstacle. In addition, the total potential field value generated is also getting bigger. When the repulsive gain value is greater with a constant attractive gain value, the potential repulsive field around the obstacle is getting bigger. The greater the potential repulsive field value, the smaller the total potential field value for the I-APF algorithm.

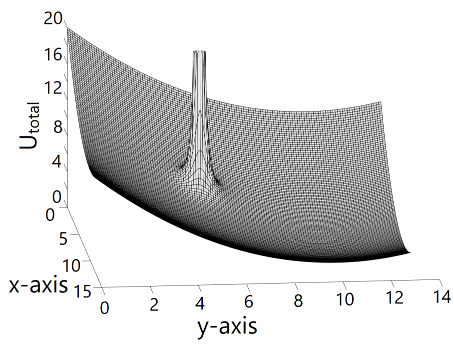

(a) T-APF

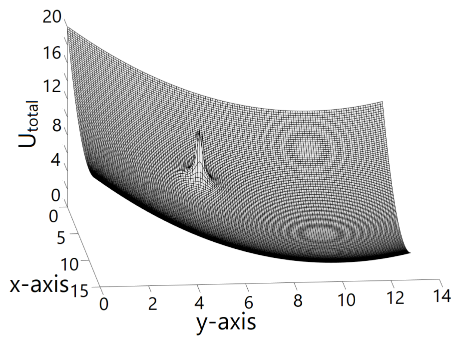

(b) I-APF

Fig. 2. Comparison of T-APF and I-APF potential field

Apart from the attractive and repulsive gain parameters, the main parameter that influences the I-APF algorithm is *m*. The value of *m* must be positive to function as an activation function of the repulsive potential field. The formation of the sigmoid function instead of the branching function depends on the value of *m*. The greater the value of *m* has an impact on the increase in the value of the potential field around the obstacle, which is *r*. Changes in the value of the potential field that is influenced by the obstacle will be more visible at large *m* values. The smaller the *m* value causes the distribution of the repulsive potential field generated by the obstacle to be more evenly distributed so that the change in the value of the potential field as a whole is getting smoother.

A. *Design of The Auxiliary Function* (v)

One type of local minimum problem is symmetrically aligned robot-obstacle-goal (SAROG). SAROG occurs because robots, obstacles, and goals are in a straight line that causes deadlock conditions. Local minimum problems can be solved using three approaches, that are local minimum avoidance (LMA), local minimum escaping (LME), and local minimum removal (LMR) [27]. In the LME approach, when the robot is trapped in a minimum local condition, some escape mechanism is triggered so that the robot moves away from the minimum local point and is possible to reach the target again. The main weakness of LME is the fact that LME cannot avoid or prevent the existence of a minimum locale so as to produce an inefficient path until the target is reached. However, due to the relatively light computation and the fact that no prior information about the environment is needed, the LME approach is still commonly used.

In this study, the LME approach is used to direct the robot away from the local minimum conditions by adding an auxiliary function (v) in the total potential force. This function is influenced by the magnitude of the force on the x-axis and y-axis. Therefore, the functions F_x and F_y in (8) and (9) are explained in more detail in (16) and (17).

$$F_x(q) = -\xi(x - x_g) - \left[\frac{0.5\eta(x_o - x)}{S_{or}^3(1 + e^{m(S_{or}-r)})} + \frac{0.5\eta m(x_o - x)}{S_{or}^2(1 + e^{m(S_{or}-r)})^2}\right] \quad (16)$$

$$F_y(q) = -\xi(y - y_g) - \left[\frac{0.5\eta(y_o - y)}{S_{or}^3(1 + e^{m(S_{or}-r)})} + \frac{0.5\eta m(y_o - y)}{S_{or}^2(1 + e^{m(S_{or}-r)})^2}\right] \quad (17)$$

The strategy to escaping local minimum conditions is to make a limitation that the total potential force in the y-axis must be n times the total value of potential force in the x-axis. In Fig. 3, it can be seen that the large potential forces on the x-axis and y-axis up to the deadlock conditions achieved in step 650. In the proposed method, if the value of the total potential force on the y-axis is less than n times the value of the total potential force in the x-axis, then the auxiliary function of v will be active. Here we set the value of v according to equation (18)

$$v = \frac{dU_{rep.i}(q)}{dx}\left(\frac{1}{1 + e^{nF_x - F_y}}\right) \quad (18)$$

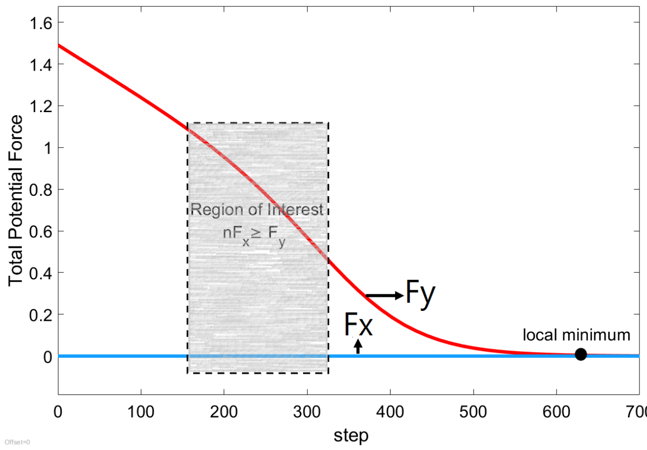

Fig. 3. Region of interest in total potential force

where n is the tuning parameter the function v is added to the y-axis potential force (F_y), so equation (17) becomes (19).

$$F_{ynew}(q) = -\xi(y - y_g) - \left[\frac{0.5\eta(y_o - y)}{S_{or}^3(1 + e^{m(S_{or}-r)})} + \frac{0.5\eta m(y_o - y)}{S_{or}^2(1 + e^{m(S_{or}-r)})^2}\right] + v \quad (19)$$

The motion planning produced by I-APF will be affected by v. Modification of the direction of the force produced based on (16) and (17) compared to (16) and (19) can be seen in Fig. 4. Using this method, when the total force in the y-axis less than the n total force in the x-axis, the robot will move with a smaller angle (α_{new}).

B. *Design of The Adaptive Distance and The Repulsive Gain*

Based on Fig. 5, the GNRON problem occurs when $S_{og} < r$. Therefore, the modification will be done by making the distance parameter r to be r_{new} based on distance S_{og}. In principle, this method is used to produce adaptive r_{new} and η_{new} values based on the distance between obstacle and goal. The equation of r_{new} dan η_{new} can be seen in (20) dan (21). The parameters n is the tuning parameters.

$$r_{new} = \frac{r}{1 + e^{n(r - S_{og})}} \quad (20)$$

$$\eta_{new} = \begin{cases} \eta & \text{if } r \leq S_{og} \\ \frac{\eta r_{new}}{r} & \text{if } r > S_{og} \end{cases} \quad (21)$$

Fig. 6 shows the relationship between r_{new} and the distance of the obstacle to the goal distances. From Fig. 6, it

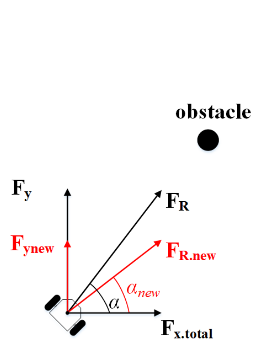

Fig. 4. Potential force modification

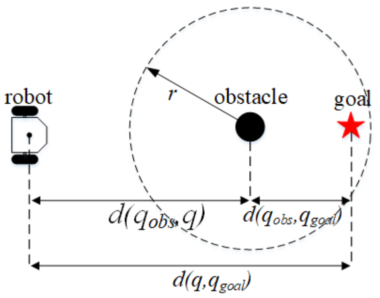

Fig. 5. GNRON problem

can be seen that the new distance produced is getting smaller when $S_{og} < r$. Fig. 6 shows the relationship between the value of η_{new} and the distance of the robot to the obstacle. At great distances the value of η_{new} is equal to the value of η. However, when the robot is close to the obstacle which is under the influence of GNRON, the value of η_{new} will be smaller. Therefore, the repulsive potential force in (15) changes to equation (22). The I-APF path planning algorithm flowchart can be seen in Fig. 7.

$$\begin{aligned} F_{rx}(q) &= -\frac{0.5\eta_{new}(x_o - x)}{S_{or}^3(1+e^{m(S_{or}-r_{new})})} - \frac{0.5m\eta_{new}(x_o - x)}{S_{or}^2(1+e^{m(S_{or}-r_{new})})^2} \\ F_{ry}(q) &= -\frac{0.5\eta_{new}(y_o - y)}{S_{or}^3(1+e^{m(S_{or}-r_{new})})} - \frac{0.5m\eta_{new}(y_o - y)}{S_{or}^2(1+e^{m(S_{or}-r_{new})})^2} \end{aligned} \tag{22}$$

IV. Result and Discussion

This study will simulate different environments to prove the I-APF algorithm in solving minimum local problems. Evaluation is done by looking at the traveling distance (D_{trav}) and the goal reachability distance error (E_{rg}) according to equations (23) and (24). D_{trav} is obtained from the amount of distance traveled to reach the target. E_{rg} is obtained from the closest distance generated between the goal and the last position of the robot (x_{end},y_{end}).

$$D_{trav} = \sum_{i=1}^{N} \sqrt{(x_{new}-x)^2 + (y_{new}-y)^2} \tag{23}$$

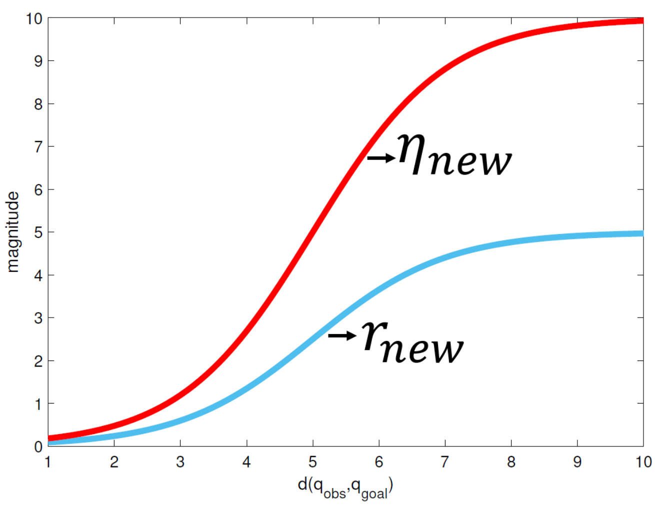

Fig. 6. Corresponding between η_{new} and r_{new} to distance r

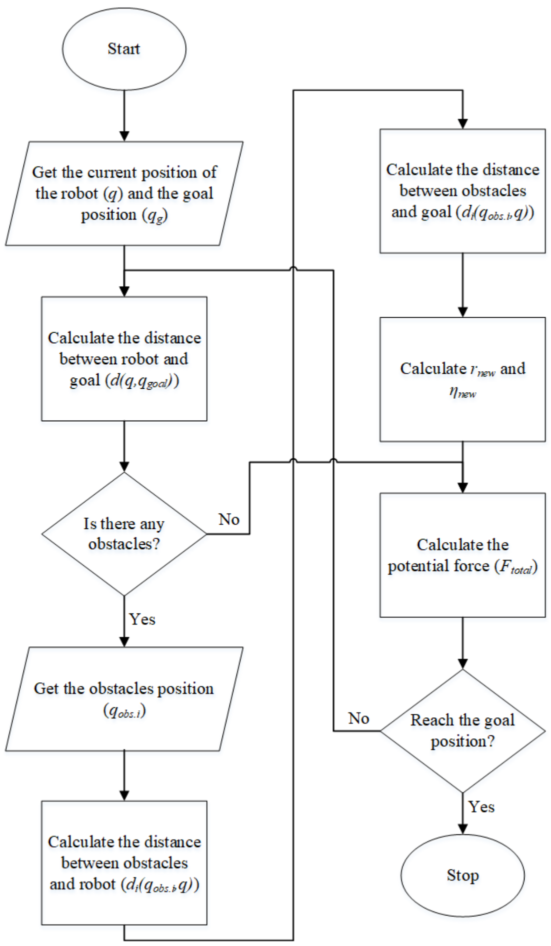

Fig. 7. Flowchart of I-APF path planning algorithm

TABLE I
PARAMETERS OF THE TEST

Env.	ξ	η	r	n	c
E1	0.15	2	4	3	0.01
E2	0.4	2	4	2	0.01
E3	0.65	2	4	2	0.01
E4	0.5	2	3	1	0.01
E5	0.15	2	3	3	0.01
E6	0.21	2	3	3	0.01

$$E_{rg} = \sqrt{(x_{end}-x_g)^2 + (y_{end}-y_g)^2} \tag{24}$$

The I-APF path planning algorithm will be tested in several environments explain in Table II. Some parameters used for testing have also been described in Table I. All tests use the same repulsive gain parameter (η) and attractive gain parameter (ξ) values. The E_{rg} tolerance (t) used throughout the test is 0.01. Environment E1 and E2 use the value of r = 4, while E3-E6 uses the value of r = 3. All of the environments start to move from (0,5) towards the goal at (10,5).

Fig. 8 (a) shows that I-APF succeeded in generating a collision-free path on E1. E1 represents a SAROG problem where the initial position, obstacle, and goal lie in a straight line. The robot will fail when the auxiliary function is not active. Fig. 8 (b) shows that in the 400th iteration, the values of F_x and F_y are zero. This means the robot has reached a local minimum condition and made the path stop at that

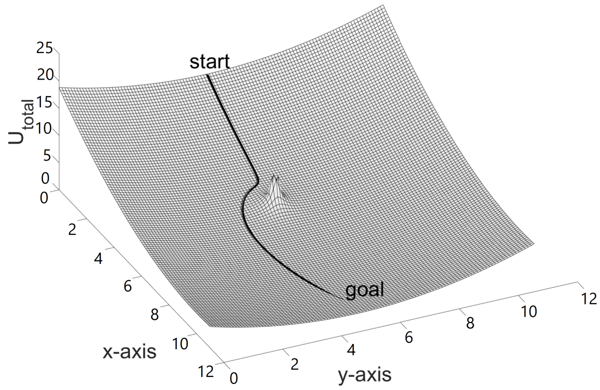

(a) Trajectory of Environment 1

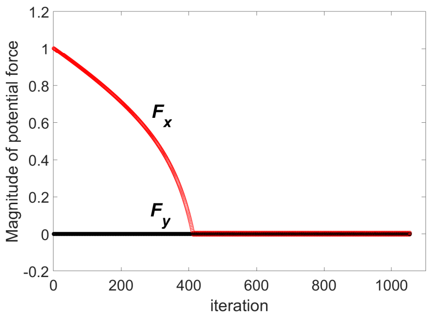

(b) Potential force of E1 without v

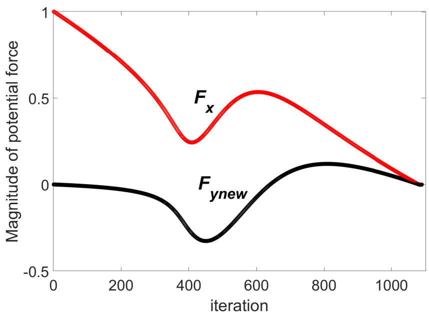

(c) Potential force of E1 with v

Fig. 8. Test result of Environment 1

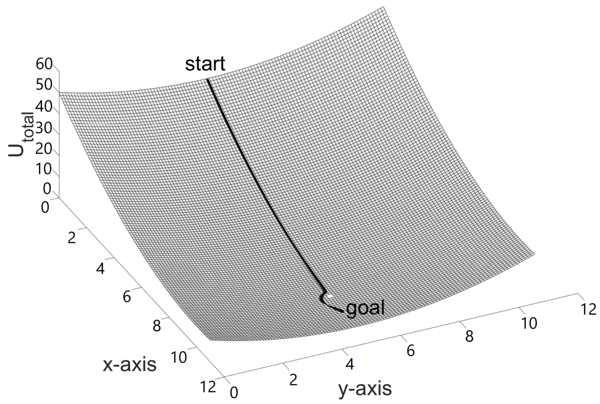

(a) Trajectory of Environment 2

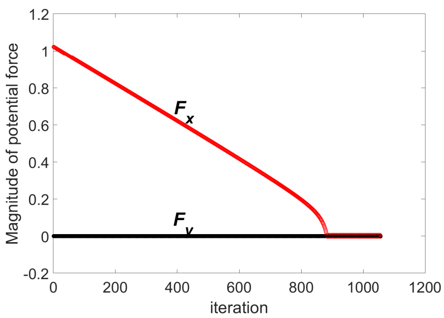

(b) Potential force of E2 without v

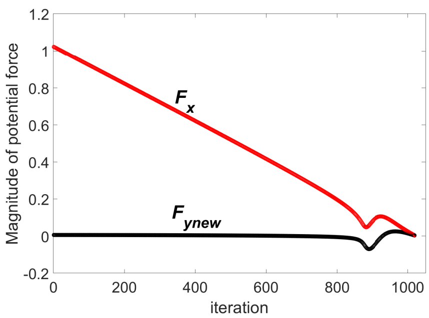

(c) Potential force of E2 with v

Fig. 9. Test result of Environment 2

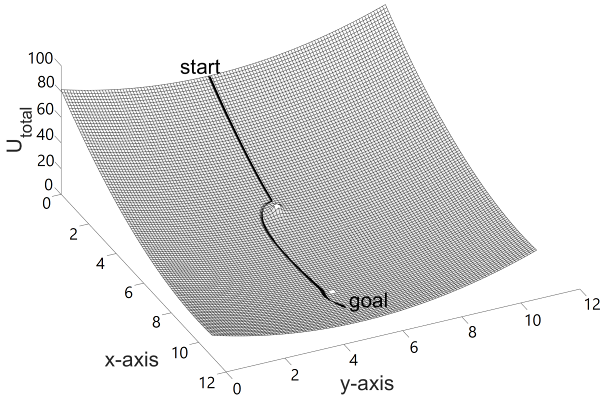

(a) Trajectory of Environment 3

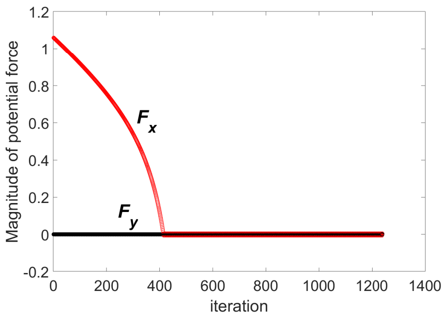

(b) Potential force of E3 without v

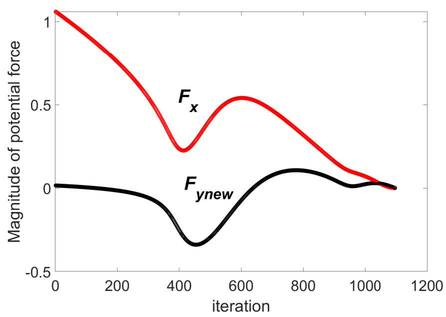

(c) Potential force of E3 with v

Fig. 10. Test result of Environment 3

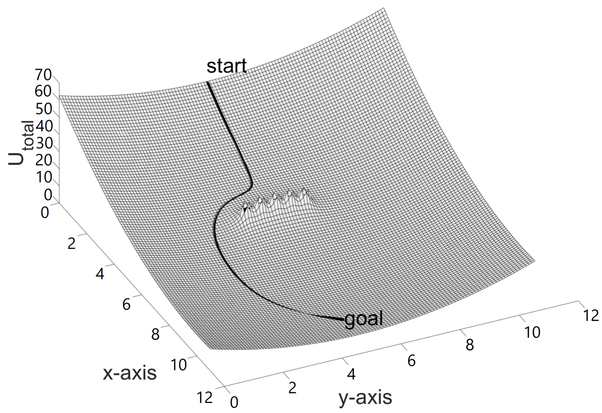

(a) Trajectory of Environment 4

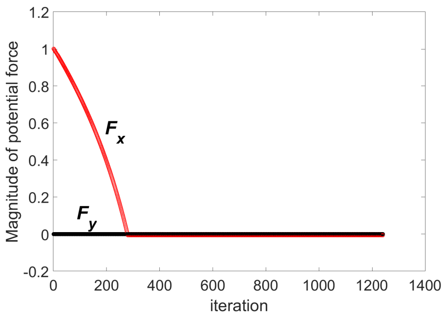

(b) Potential force of E4 without v

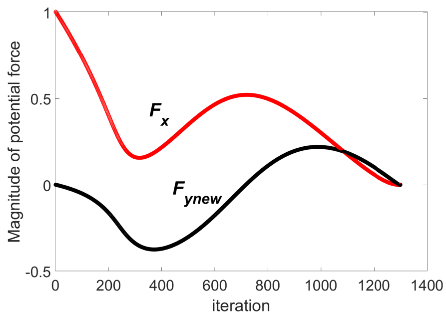

(c) Potential force of E4 with v

Fig. 11. Test result of Environment 4

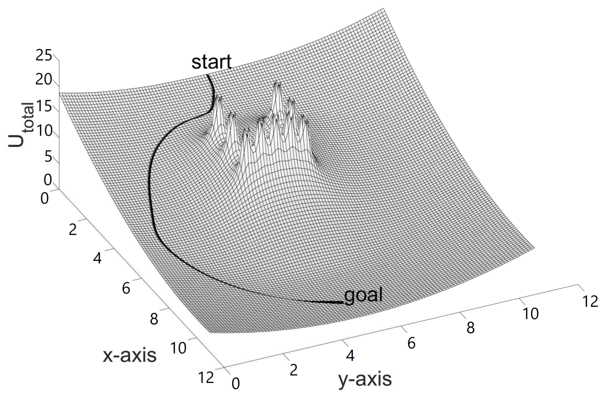

(a) Trajectory of Environment 5

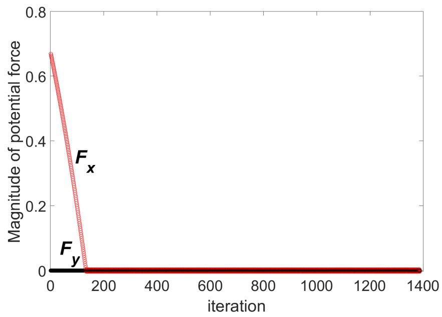

(b) Potential force of E5 without v

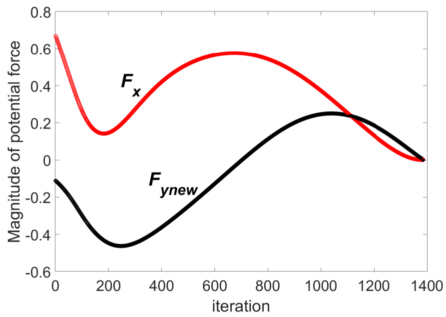

(c) Potential force of E5 with v

Fig. 12. Test result of Environment 5

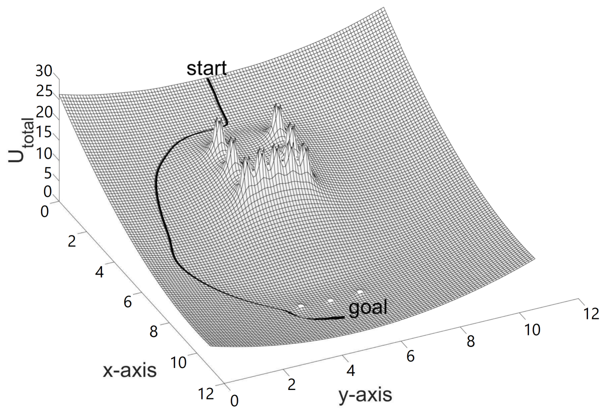

(a) Trajectory of Environment 6

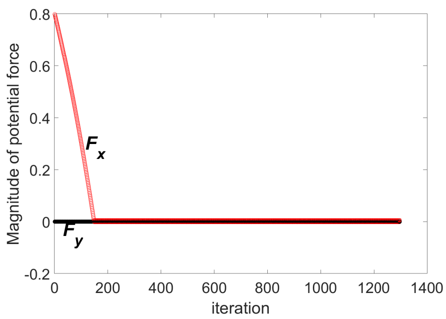

(b) Potential force of E6 without v

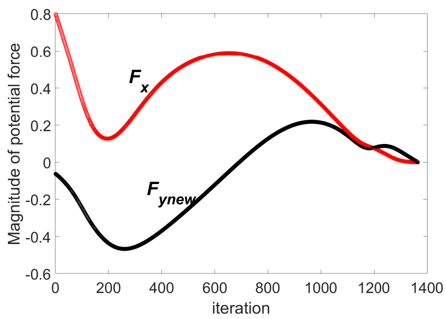

(c) Potential force of E6 with v

Fig. 13. Test result of Environment 6

condition. The values of F_x and F_y show zero values, which means that the attractive force received by the robot is the same as its repulsive force. Fig. 8 (c) shows the effect of the auxiliary function in solving SAROG problems. The value of F_x and F_ynew in the 400th iteration produces a new value that deflects the path away from the obstacle. The resulting path reaches the goal position with t = 0.01 in the 1020th iteration. The resulting E_{rg} value is 0.0016.

Environment E2 shows GNRON problems where the obstacle is close to the goal. Fig. 9 (a) shows that the η_{new} value becomes smaller than η. It is also indicated by the height of the resulting potential field. When the APF algorithm does not apply the auxiliary function, the deadlock condition is reached in 900th iterations. The I-APF algorithm that uses an auxiliary function generates a new F_x and F_ynew force that deflects the path away from a deadlock condition.

Environment E3 represents the combination problems of SAROG and GNRON. Fig.10 (a) shows that I-APF succeeded in producing a collision-free path similar to E1. The difference between Fig.8 (c) and Fig.10 (c) is in the avoidance of GNRON in 900th iterations. The resulting η_{new} and r_{new} values in $q_{obs.2}$= [9,5] are 0.0949 and 0.1897.

A more complex form of the obstacle is shown in E4. E4 represents the SSOD problem with the obstacle arranged parallel in front of the robot. According to Fig.11 (a), the auxiliary function plays an important role in solving SSOD problems. The I-APF algorithm is able to produce a path that is able to avoid the symmetric obstacle located in front of the robot. Based on Fig.11 (b) and (c), the auxiliary function is active in 280th iterations. In accordance with (19), the direction of the path will go to the right of the obstacle because the F_{ynew} value is smaller than F_y. The resulting E_{rg} value is 0.0059.

E5 represents the SSOD problem with the U-shape obstacle. Combined SSOD and GNRON problems are represented in the E6 environment. There are several symmetric obstacles that are near the goal. The ηnew values for each obstacle near the goal are 0.3399, 0.2384, and 0.3399. According to Fig. 12 (a) and Fig. 13 (a), I-APF utilizes an auxiliary function to avoid two adjacent obstacles and form SSOD problems. After that, the obstacle near the goal is avoided by utilizing adaptive r_{new} and η_{new} according to equations (6) and (20).

TABLE II
ENVIRONMENT SETUP

Env.	Initial Position (x_i, y_i)	Obstacle Position (x_o, y_o)	Goal Position (x_g, y_g)
E1	(0,5)	(5,5)	(10,5)
E2	(0,5)	(9,5)	(10,5)
E3	(0,5)	(5,5);(9,5)	(10,5)
E4	(0,5)	(5,4);(5,4.5);(5,5) ;(5,5.5);(5,6)	(10,5)
E5	(0,5)	(3,4);(4,4);(5,4) ;(5,6);(5,5);(5,5.5) ;(5,4.5); (4,6); (3,6)	(10,5)
E6	(0,5)	(3,4);(4,4);(5,4) ;(5,4.5);(5,5);(5,5.5) ;(5,6);(4,6);(3,6) ;(9,5);(9,4);(9,6)	(10,5)

According to Fig. 12 (b) and Fig. 13 (b), if the auxiliary function is not active, the deadlock condition will be reached in the 180th iteration. However, Fig. 12 (c) and Fig. 13 (c) shows that I-APF is able to avoid deadlock conditions using the auxiliary function in equation (18).

TABLE III
RESULT OF THE TESTS

Env.	Step	m	E_{rg}	D_{trav}
E1	1072	0.1	0.0016	10.72
E2	1020	0.1	0.0098	10.20
E3	1038	0.1	0.0091	10.38
E4	1197	3.0	0.0059	11.97
E5	1407	4.0	0.0098	14.07
E6	1422	6.0	0.0099	14.22

Based on the experiments, a summary of the experimental results can be seen in Table III. The average of D_{trav} and E_{rg} values generated in all of the environments were 11.93 and 0.0077. The error generated by all tests is less than the specified tolerance limit of 0.01. It shows all the results towards the goal as an equilibrium point. In addition, based on the resulting image, the paths generated in all environments indicate that the proposed path planning algorithm can produce a safe path without crashing into obstacles between the initial and the goal.

V. CONCLUSION

The multi-local minimum problem-solving approach has been described in this study. The main parameter that is seen is the success rate of the I-APF algorithm in achieving the goal, which is represented by E_{rg} and distance traveled (D_{trav}). From the test results, it can be seen that changes in the value of m affect the value of E_{rg}. The value of E_{rg} can be reached based on the predefined tolerance value. In this study, the average E_{rg} value with a tolerance of 0.01 was 0.0077. From all tests, the value of the shortest distance between the initial position and the goal is 10. The average of the total trajectory (D_{trav}) generated by the I-APF algorithm is 11.93. According to the results, it shows that the I-APF algorithm can solve local minimum problems in the form of single local minimum problems and multi-local minimum problems.

REFERENCES

[1] H. Y. Zhang, W. M. Lin, and A. X. Chen, "Path planning for the mobile robot: A review," *Symmetry*, vol. 10, no. 10, pp. 450–466, Oct 2018.

[2] T. Weerakoon, K. Ishii, and A. A. F. Nassiraei, "An artificial potential field based mobile robot navigation method to prevent from deadlock," *Journal of Artificial Intelligence and Soft Computing Research*, vol. 5, no. 3, pp. 189 – 203, 2015.

[3] T. T. Mac, C. Copot, D. T. Tran, and R. De Keyser, "Heuristic approaches in robot path planning: A survey," *Robotics and Autonomous Systems*, vol. 86, pp. 13–28, 2016.

[4] B. Patle, Ganesh, A. Pandey, D. Parhi, and A. Jagadeesh, "A review: On path planning strategies for navigation of mobile robot," *Defence Technology*, vol. 15, no. 4, pp. 582 – 606, 2019.

[5] M. N. Zafar and J. Mohanta, "Methodology for path planning and optimization of mobile robots: A review," *Procedia Computer Science*, vol. 133, pp. 141 – 152, 2018.

[6] S. Garrido and L. Moreno, *Mobile Robot Path Planning using Voronoi Diagram and Fast Marching*. IGI Global Books, May 2015.

[7] M. Zimmermann and C. König, “Integration of a visibility graph based path planning method in the act/fhs rotorcraft,” *CEAS Aeronautical Journal*, vol. 7, 06 2016.

[8] R. Gonzalez, M. Kloetzer, and C. Mahulea, “Comparative study of trajectories resulted from cell decomposition path planning approaches,” in *2017 21st International Conference on System Theory, Control and Computing (ICSTCC)*, 2017, pp. 49–54.

[9] O. Khatib, “Real-time obstacle avoidance for manipulators and mobile robots,” in *Proceedings. 1985 IEEE International Conference on Robotics and Automation*, vol. 2, 1985, pp. 500–505.

[10] H. H. Triharminto, O. Wahyunggoro, T. B. Adji, A. Cahyadi, and I. Ardiyanto, “Local information using stereo camera in artificial potential field based path planning,” *IAENG International Journal of Computer Science*, vol. 44, no. 3, pp. 316–326, 2017.

[11] A. Alomari, W. Phillips, N. Aslam, and F. Comeau, “Dynamic fuzzy-logic based path planning for mobility-assisted localization in wireless sensor networks,” *Sensors*, vol. 17, p. 1904, Aug 2017.

[12] B. Patle, D. Parhi, J. Anne, and S. K. Kashyap, “Matrix-binary codes based genetic algorithm for path planning of mobile robot,” *Computers and Electrical Engineering*, vol. 67, Dec 2017.

[13] S. Yang and M. Meng, “An efficient neural network approach to dynamic robot motion planning,” *Neural Networks*, vol. 13, pp. 143–148, Mar 2000.

[14] J. Borenstein and Y. Koren, “Real-time obstacle avoidance for fast mobile robots,” *IEEE Transactions on Systems, Man, and Cybernetics*, vol. 19, no. 5, pp. 1179–1187, 1989.

[15] W. J. Yim and J. B. Park, “Analysis of mobile robot navigation using vector field histogram according to the number of sectors, the robot speed and the width of the path,” in *2014 14th International Conference on Control, Automation and Systems (ICCAS 2014)*, 2014, pp. 1037–1040.

[16] Y. Zhu, T. Zhang, and J. Song, “An improved wall following method for escaping from local minimum in artificial potential field based path planning,” in *Proceedings of the 48h IEEE Conference on Decision and Control (CDC) held jointly with 2009 28th Chinese Control Conference*, 2009, pp. 6017–6022.

[17] E. F. Mohamed, K. El-Metwally, and A. R. Hanafy, “An improved tangent bug method integrated with artificial potential field for multi-robot path planning,” in *2011 International Symposium on Innovations in Intelligent Systems and Applications*, 2011, pp. 555–559.

[18] J. Choi, “A potential field and bug compound navigation algorithm for nonholonomic wheeled robots,” in *2012 First International Conference on Innovative Engineering Systems*, 2012, pp. 166–171.

[19] P. Mohanty and D. Parhi, “Controlling the motion of an autonomous mobile robot using various techniques: a review,” *Journal of Advanced Mechanical Engineering*, vol. 1, pp. 24–39, Jan 2013.

[20] F. Bounini, D. Gingras, H. Pollart, and D. Gruyer, “Modified artificial potential field method for online path planning applications,” in *2017 IEEE Intelligent Vehicles Symposium (IV)*, Jun 2017, pp. 180–185.

[21] U. Orozco-Rosas, O. Montiel, and R. Sepúlveda, “Mobile robot path planning using membrane evolutionary artificial potential field,” *Applied Soft Computing*, vol. 77, pp. 236 – 251, 2019.

[22] T. D. Chen and Y. Y. Huang, “Non-trap artificial potential field based on virtual obstacle,” in *2019 IEEE 16th International Conference on Networking, Sensing and Control (ICNSC)*, 2019, pp. 275–280.

[23] S. M. Hosseini Rostami, A. Kumar, J. Wang, and X. Liu, “Obstacle avoidance of mobile robots using modified artificial potential field algorithm,” *EURASIP Journal on Wireless Communications and Networking*, vol. 2019, Mar 2019.

[24] J. Lee, Y. Nam, and S. Hong, “Random force based algorithm for local minima escape of potential field method,” in *2010 11th International Conference on Control Automation Robotics Vision*, 2010, pp. 827–832.

[25] S. S. Ge and Y. J. Cui, “New potential functions for mobile robot path planning,” *IEEE Transactions on Robotics and Automation*, vol. 16, no. 5, pp. 615–620, 2000.

[26] H. H. Triharminto, O. Wahyunggoro, T. B. Adji, and A. I. Cahyadi, “An integrated artificial potential field path planning with kinematic control for nonholonomic mobile robot,” *International Journal on Advanced Science, Engineering and Information Technology*, vol. 6, no. 4, pp. 410–418, 2016.

[27] N. S. F. Doria, E. O. Freire, and J. C. Basilio, “An algorithm inspired by the deterministic annealing approach to avoid local minima in artificial potential fields,” in *2013 16th International Conference on Advanced Robotics (ICAR)*, 2013, pp. 1–6.

Riky Dwi Puriyanto is currently a doctoral student at Department of Electrical Engineering and Information Engineering, Universitas Gadjah Mada. He obtained his bachelor degree from Department of Electrical Engineering and Information Engineering, Faculty of Engineering, Universitas Gadjah Mada, Indonesia in 2010. Later he got his master degree from Department of Electrical Engineering and Information Engineering, Faculty of Engineering, Faculty of Engineering, Universitas Gadjah Mada, Indonesia in 2014. He is currently lecturer in Department of Electrical Engineering, Universitas Ahmad Dahlan. His research interest involves robotics and industrial automation.

Oyas Wahyunggoro was born in Yogyakarta, Indonesia. He received the undergradute degree (Ir) in electrical engineering from Universitas Gadjah Mada (UGM), Indonesia, Feb 1993, the master degree (M.T.) in Electrical Engineering from Universitas Gadjah Mada (UGM), Yogyakarta, May 2001, and Ph.D. degree from Universitas Teknologi PETRONAS, Malaysia, Oct 2011. Currently, he is an Associate Professor with the Department of Electrical and Information Engineering, Engineering Faculty, Universitas Gadjah Mada, Indonesia. His major research focus is applying fuzzy logic controller on UAV as surveilence of city and land condition.

Adha Imam Cahyadi obtained his bachelor degree from Department of Electrical Engineering, Faculty of Engineering, Universitas Gadjah Mada in 2002. Later he got his master in Control Engineering from KMITL in 2005, Thailand, and Doctor of Engineering from Tokai University Japan in 2008. He is curently lecturer in Department of Electrical and Information Engineering, Universitas Gadjah Mada. His research areas involves mechanical control systems, telemanipulation systems, and Unmanned Aerial Vehicles.